XLI CILAMCE
XLI Ibero-Latin American Congress on Computational Methods in Engineering
16-19 November, 2020 FOZ DO IGUAÇU PARANÁ – BRAZIL

Dynamic modeling of a liquid rocket engine turbo pump rotor

Sâmela Fernandes Pereira de Lima[1], Carlos d'Andrade Souto[1]

[1]*Aeronautical engineering course, Dept. of Mechanical Engineering, University of Taubaté*
Rua Daniel Danelli, s/n, 12060-440, Taubaté, SP, Brazil
samelafplima@hotmail.com
[2]*Division of Integration and Tests, Institute of Aeronautical and Space, Department of Science and Aerospace Technology*
Praça Mal. Eduardo Gomes, 50 - Vila das Acácias CEP: 1222890 , São José dos Campos, SP ,Brazil
soutocds@fab.mil.br

Abstract. Liquid propelled rocket engines present many advantages over its solid propelled counterpart: the possibility of shutdown and re-ignition in flight and the fact that they are more efficient (greater specific impulse). For these reasons, they are used in most satellite launching rockets. In a liquid propellant rocket engine, the oxidizer and fuel must be injected under high pressure into the combustion chamber. This can be achieved by using pressurized tanks. This solution is technologically simpler and less costly but significantly limits the injection pressures of propellants. To obtain more powerful engines, propellants must be injected at higher pressures into the combustion chamber. This is done using a turbo pump, a high-capacity pump powered by a gas turbine. Turbo pumps operate at high angular speeds (tens of thousands of rpm) and undergo intense dynamic loads in flight, in addition to the dynamic loads intrinsic to the operation of rotating machines. Therefore, the dynamic behavior of this type of system must be evaluated at the design stage. In this work, the transverse displacements of a turbo pump rotor are analyzed using routines developed in the numerical computation software Octave. The mathematical model developed considers the rotor shaft flexible and rigid disks. The axis is modeled using finite elements and point masses and inertias are used to represent the disks. Campbell's diagram, response to unbalance and forces applied on bearing are obtained. The influence of bearings positioning on the rotor unbalance response is studied.

Keywords: Rotordynamics, turbo-pump, finite-elements

1 Introduction

In liquid propellant rocket engines turbo pumps are used to inject fuel and oxidant in the combustion chamber that operates at high pressure allowing higher thrusts than obtained with the pressurized tank pumping system as pointed out by Sutton and Biblarz [1]. In order to inject large flows at high pressure and have a light structure the turbo pump needs to operate at high speed. In the conception phase it is important to assess the influence of design parameters on the dynamic response of the rotor in transverse vibrations, mainly in a system where the housing - rotor clearances are quite small as discussed by Porto [2]. The Monte Carlo method can be a useful tool to evaluate the effect of uncertainties in rotors as done by Costa et al. [3].

In this work a rotordynamic analysis of a turbo pump rotor-bearing system was carried out. The natural frequencies, the response to the unbalance and the forces applied by the rotor on the bearings as functions of the speed of rotation were obtained. The influence of shifts in the positioning of the bearings along the shaft in the response to the unbalance was evaluated by using a Monte Carlo simulation. Since the model analyzed has a few tens of degrees of freedom, it becomes possible to use the Monte Carlo method to obtain optimal design parameters within a limited range.

2 Rotor Equations

The mathematical model considered for the rotor-bearing system consists of a flexible shaft with point masses representing the disks (assumed rigid) and suspended by two roller bearings treated as horizontal and vertical stiffness with damping. The shaft is modelled by beam elements (with two nodes), the disks by point elements (one node) and the bearings by vertical and horizontal springs and dampers. The equations of motion of all elements are assembled to form the rotor – bearing system equation of motion.

2.1 Shaft Element

The equation of motion of a shaft finite element presented by Lalanne [4] is:

$$[M_s^e]\{\ddot{x}_s^e(t)\} - \Omega[G_s^e]\{\dot{x}_s^e(t)\} + [[K_s^e]\{x_s^e(t)\} = \{f_s^e(t)\} \tag{1}$$

Where $[M_s^e]$ is the mass matrix; $[G_s^e]$ is the gyroscopic matrix; $[K_s^e]$ is the stiffness matrix; $\{\ddot{x}_s^e(t)\}, \{\dot{x}_s^e(t)\}$ and $\{x_s^e(t)\}$ are the acceleration, velocity and displacement nodal vectors respectively; $\{f_s^e(t)\}$ is the nodal forces vector; and Ω is the rotation speed. The nodal displacements vector is: $\{x_s^e\} = \{u_1\ w_1\ \theta_1\ \psi_1\ \ u_2\ w_2\ \theta_2\ \psi_2\}$, where *u* and *w* are the horizontal and vertical displacements and θ and ψ are the angular displacements on each node.

2.2 Disks

The dynamic equation for a disk element is:

$$[M_d^e]\{\ddot{x}_d^e(t)\} - \Omega[G_d^e]\{\dot{x}_d^e(t)\} = \{f_d^e(t)\} \tag{2}$$

Where $[M_d^e]$ is the mass matrix; $[G_d^e]$ is the gyroscopic matrix; $\{\ddot{x}_d^e(t)\}$ and $\{\dot{x}_d^e(t)\}$ are the acceleration and velocity nodal vectors respectively; and $\{f_d^e(t)\}$ is the forces nodal vector. The nodal degrees of freedom vector is $\{x_d^e\} = \{u \quad w \quad \theta \quad \psi \quad\}$.

2.3 Bearings

The matrix equation for the bearings is given by:

$$[C_b^e]\{\dot{x}_b^e(t)\} - [K_b^e]\{x_b^e(t)\} = \{f_b^e(t)\} \tag{3}$$

Where $[C_b^e]$ is the damping matrix; $[K_b^e]$ is the stiffness matrix; $\{\dot{x}_b^e(t)\}$ and $\{x_b^e(t)\}$ are the velocity and displacement nodal vectors respectively and has the same given by Eq. (5)) and $\{f_b^e(t)\}$ represents the nodal forces vector.

2.4 Rotor-bearing system

With the dynamic matrix equations presented above for the shaft, disks and bearings is possible to assemble those equations in a single matrix equation to obtain the system's global matrix equations:

$$[M]\{\ddot{x}(t)\} + [D(\Omega)]\{\dot{x}(t)\} + [K]\{x(t)\} = \{f(t)\} \tag{4}$$

Where $[M]$ is the mass matrix; $[D(\Omega)]$ is given by $[D(\Omega)] = ([C] - \Omega[G])$; $[C]$ is the damping matrix; $[G]$ is the gyroscopic matrix; $[K]$ is the stiffness matrix; $\{\ddot{x}(t)\}$, $\{\dot{x}(t)\}$ and $\{x(t)\}$ represents respectively the acceleration, velocity and displacement nodal vectors; and $\{f(t)\}$ represents the nodal force vector.

3 Analysis

3.1 Unbalance Response

For real rotors some unbalance must be included in the model due to the difference between geometric center and center of mass. The unbalance is defined by a mass *m* placed at a distance *e* from the center of the disk. The forces applied on the rotor due to the unbalance and the corresponding rotor response can be decomposed in sine and cosine components:

$$\{F\} = \{F_s\}sin(\Omega t) + \{F_c\}cos(\Omega t) \tag{5}$$

$$\{Q\} = \{Q_S\}sin(\Omega t) + \{Q_C\}\cos(\Omega t) \tag{6}$$

Where:

$$\{F_S\} = \{u_1\ w_1\ \theta_1\ \psi_1 \ldots . u_n\ w_n\ \theta_n\ \psi_n\}^T = \{me\Omega^2\ \sin(\Omega t)\quad 0\quad 0 \ldots \ldots .0\ \ 0\ \ 0\ 0\}^T \tag{7a}$$

$$\{F_C\} = \{u_1\ w_1\ \theta_1\ \psi_1 \ldots . u_n\ w_n\ \theta_n\ \psi_n\}^T = \{0\quad me\Omega^2\ cos(\Omega t)\quad 0\ \ 0 \ldots .0\ \ 0\ \ 0\ 0\}^T \tag{7b}$$

With the sine and cossine components of excitation and the response for the external force, the vectors $\{Q_s\}$ and $\{Q_c\}$ are obtained by doing:

$$\begin{Bmatrix} Q_S \\ Q_c \end{Bmatrix} = \begin{bmatrix} [K]-\Omega^2[M] & -\Omega[D(\Omega)] \\ \Omega[D(\Omega)] & [K]-\Omega^2[M] \end{bmatrix}^{-1} \begin{Bmatrix} F_s \\ F_c \end{Bmatrix} \tag{8}$$

Once the displacements and transversal speeds of the shaft nodes in the bearings have been determined and knowing the stiffness and damping of the bearings, it is possible to determine the forces applied by the rotor on the supports.

3.2 Eigenvalue Analysis

In order to use algorithms for symmetric matrices, it is useful to transform eq.(4) a second order differential matrix equation into a first order differential equation in the space-state format:

$$[A]\{\dot{q}\} + [B]\{q\} = \{F\} \tag{9}$$

Where:

$$[A] = \begin{bmatrix} [M] & [0] \\ [0] & -[K] \end{bmatrix} \qquad [B] = \begin{bmatrix} [D(\Omega)] & [K] \\ [K] & [0] \end{bmatrix} \qquad \{F\} = \begin{Bmatrix} \{f(t)\} \\ \{0\} \end{Bmatrix} \qquad \{q\} = \begin{Bmatrix} \dot{x}(t) \\ x(t) \end{Bmatrix} \tag{10}$$

The homogenous version of eq. (9) must be solved to obtain the natural frequencies and mode shapes of the rotor-bearing system for each value of Ω.

3.3 Sensitivity Analysis

The bearings positions, b_1 and b_2 (shown in Fig. 1), were treated as uncertain but bounded and uniform distributions for these design parameters were considered in Monte Carlo simulations. We performed the calculations for different values of b_1 and b_2 to assess the effect of modifications in the bearings positions in the rotor maximum lateral displacement due to unbalance. For dimension b_1 only a reduction (corresponding to a displacement of the bearing towards the turbine) was considered, in view of the positioning of the bearing in relation to the fuel pump. For dimension b_2, reduction and increase were considered. Both the reductions and the increases in the dimensions b1 and b2 were considered maximum variations of 10% in relation to the original b_1 and b_2 values.

4 Rotor bearings system analyzed

The rotor studied is a turbopump similar to the one analyzed by Sias et al [5]. The rotor with pumps, turbine and ball bearings (with its coordinates) is displayed in Fig. 1. A description of the shaft geometry is presented in Fig. 2.

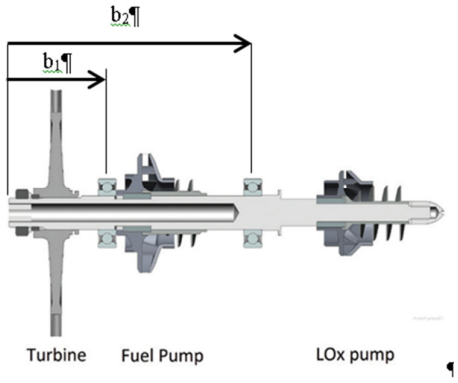

Figure 1 – Turbopump rotor (adapted from Almeida and Pagliuco [6])

The rotor operating speed is 29922,60 rpm. The shaft is made of stainless steel AISI 410 (specific mass: 7800 kg/m^3; and Young's modulus: 200 GPa). The positions of the rotor components on the shaft are presented in Tab.1. The bearings damping and stiffness properties are described in Tab.2, and the mass and inertia properties of the disks are displayed in Tab. 3. The values of unbalance masses were determined considering a G2.5 quality grade in ISO 21940-11:2016 Standard [7] and are shown in Tab.4.

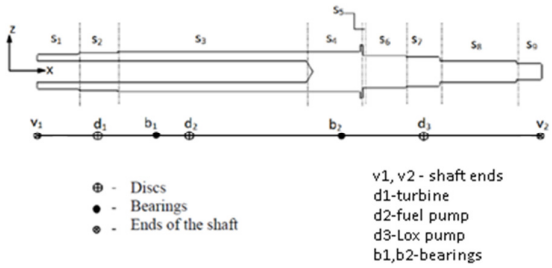

Figure 2 – Shaft geometry

Table 1 – Rotor components position

Elements	v1	b1	b2	d1 (turbine)	d2 (fuel pump)	d3 (Lox pump)
x [m]	0	0.095	0.225	L	2.7411L	6.7337L

Table 2 – Bearings properties

Bearings	Kyy [N/m]	Kzz [N/m]	Cyy [Ns/m]	Czz [Ns/m]
b1,b2	$25.48x10^6$	$25.48x10^6$	$0.5x10^3$	$0.5x10^3$

Table 3 – Disks properties

Elements	Mass [Kg]	Jx [Kg.m^2]	Jy [Kg.m^2]	Jz [Kg.m^2]
d1 (turbine)	2.379	1.082×10^{-2}	5.454×10^{-3}	5.454×10^{-3}
d2 (fuel pump)	0.17344	1.889×10^{-4}	1.0095×10^{-4}	1.0045×10^{-4}
d3 (Lox pum)	0.12466	9.1375×10^{-5}	5.0715×10^{-5}	5.0433×10^{-4}

Table 4 – Unbalance masses

Disk	Turbine	Fuel pump	Lox pump
Unbalance [g.mm]	20.8025	13.7587	7.9810

5 Results

Figures (3) and (4) shows the Campbell diagram and the unbalance responses respectively, calculated with rotation steps of 200 rpm.

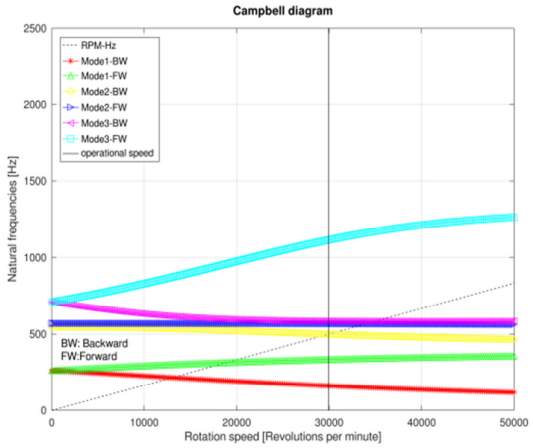

Figure 3 – Campbell diagram

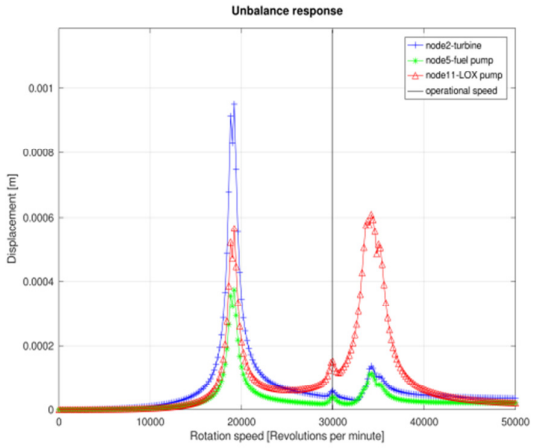

Figure 4 – Unbalance responses

One can notice that the operating speed does not match any critical speed and is placed between the first critical speed (19121 rpm) and the second one (34193 rpm). The corresponding 1st and 2nd forward modes frequencies are 318.68 Hz and 569.88 Hz. The forces applied on the bearings by the rotor are displayed in Fig. 5.

Due to the original position of bearing b_1 facing the fuel pump, as possible values for dimension b_1 only values such as $b_{1\ min} < b_{1original}$ were considered while for dimension b_2 values such that $b_{2\ min} < b_{2original} < b_{2\ max}$ (the original values of dimensions b_1 and b_2 are denoted by $b_{1original}$ and $b_{2original}$) were considered. The range of values analyzed for dimensions b1 and b2 are $b_{1\ min}=0.9b_{1original}$, $b_{2\ min}=0.9b_{2original}$ and $b_{2\ max}=1.1b_{2original}$, i.e. a decreasing or increasing of 10% of the original value. A set of 10 values were assigned to each parameter b_1 and b_2 which results in a 100 of total simulations. The unbalance responses of the Lox pump calculated for various bearings positions are shown in Fig. 6 where it can be seen that the shifts in dimensions b_1 and b_2 affect the rotation corresponding to the peak, but slightly change the shape of the curves. The curves for the fuel pump and turbine are very similar and are not shown.

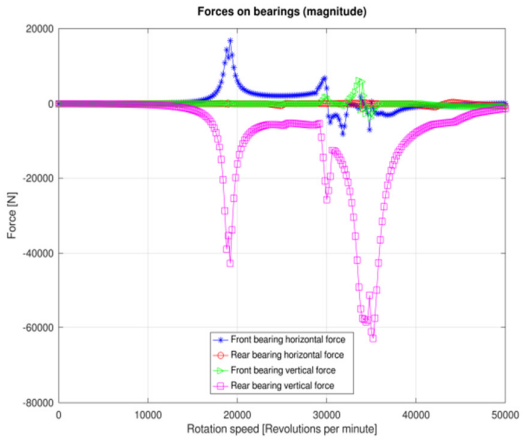

Figure 5 – Forces applied on bearings

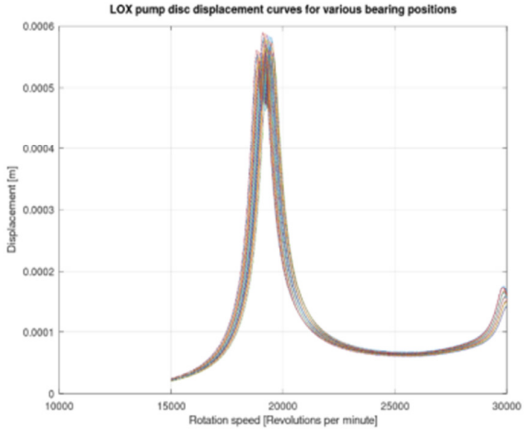

Figure 6 – Lox pump unbalance response curves for different values of b_1 and b_2

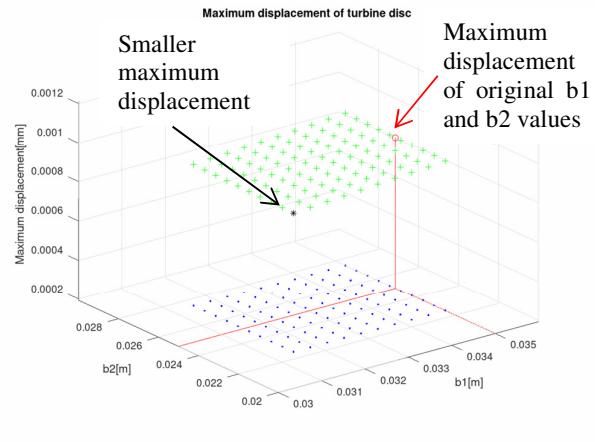

Figure 7 – Turbine maximum displacement for different values of b_1 and b_2

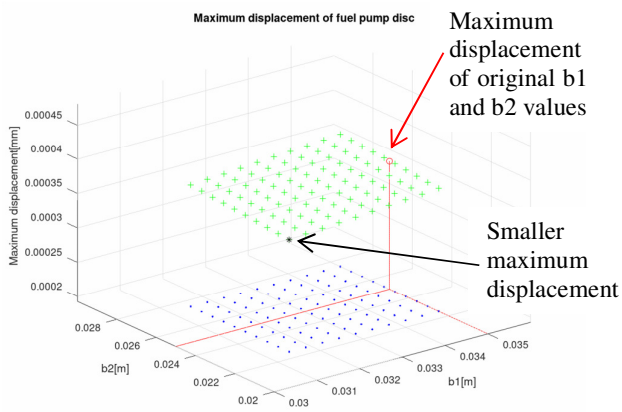

Figure 8 – Fuel pump maximum displacement for different values of b_1 and b_2

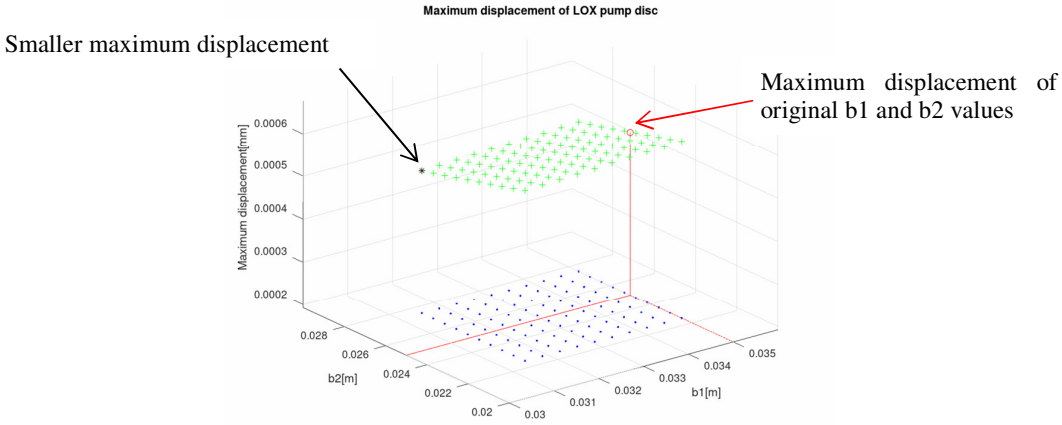

Figure 9 – Lox pump maximum displacement for different values of b_1 and b_2

The effect of changes in b1 and b2 on the value of the maximum displacement of the unbalance response can be seen in Figs 7, 8 and 9. The shifts in b1 and b2 affect the maximum displacement value very smoothly, as can be seen in the surfaces plotted in Figs 7, 8 and 9. Therefore, the use of a small number of Monte Carlo simulations was considered acceptable.

The maximum displacement varies smoothly and it is easy to obtain the pair (b1, b2) that provides the smallest maximum displacement in each disk. The effects of changes in dimensions b_1 and b_2 are summarized in Tab. 5. A decreasing of 10% and an increasing of 10% in the dimensions b1 and b2 results in a maximum decreasing of 7.35 % in the fuel pump displacement and an increasing of 12% in the Lox pump displacement. Since the Lox pump is close to one free shaft end, it should be expected that it would be more affected by the shifting in the bearings position.

Table 5 – Effect of changes in dimensions b_1 and b_2 in disks responses and bearings forces

Curve	Unity	Original peak value	Min. peak value	Min. peak value difference to the original %	Max. peak value	Max. peak value difference to the original %
Displacement (*) turbine	mm	0.970	0.901	-7.106	0.970	0.000
Displacement (*) fuel pump	mm	0.385	0.357	-7.350	0.385	0.000
Displacement (*) Lox pump	mm	0.542	0.525	-3.020	0.607	12.080

(*) Unbalance response

6 Conclusions

A simple and intuitive sensitivity analysis was able to provide useful insights about the rotor – bearing system behavior and sensitivity to some design parameters. By identifying the pair (b_1,b_2) that provides the greatest reduction in the peak unbalance displacement in the disks, a configuration of the bearing rotor system less subject to transverse vibrations can be obtained. As the model used in the analysis has only a few tens of degrees of freedom, it is quite adequate to carry out this type of study. A similar analysis considering a more complete description of the rotor – bearing system including the seals damping and stiffness properties would be a natural continuity of this work.

Acknowledgements. The authors thanks CNPq for the scholarship granted to the first author. .

Authorship statement. The authors hereby confirm that they are the sole liable persons responsible for the authorship of this work, and that all material that has been herein included as part of the present paper is either the property (and authorship) of the authors, or has the permission of the owners to be included here.

References

[1] George P. Sutton and Oscar Biblarz , *Rocket propulsion elements* John Wiley ,2001, 7th edition
[2] Bruno F. Porto "Design of the rotor assembly of a turbine pump for a liquid propulsion rocket engine", 2011, 99pp. Professional Master's Diss. in Aerospace Engineering-Instituto Tecnológico de Aeronáutica, S. J. dos Campos, in Portuguese
[3] T. N. Costa, D. F. Gonçalves, R.A. Borges "Numerical Evaluation of the effect of uncertainties in rotaiting machinery using reduced model, XXXVII Iberian Latin American Congress on Computational Methods in Engineering, BrasíliaDF-Brazil, November 6-9, 2016
[4] Michel Lalanne e Guy Ferraris "*Rotordynamics Prediction in Engineering*", Wiley 1990
[5] D.F.Sias, E. de Barros, C.d'A.Souto, D.S.Almeida, Dynamic Analysis of a Liquid Rocket Turbopump Unit", *23rd ABCM International Congress of Mechanical Engineering* December 6-11, 2015, Rio de Janeiro, RJ, Brazil
[6] D. S. Almeida, C. M. M. Pagliuco, "Development Status of L75: A Brazilian Liquid Propellant Rocket Engine", *Journal of Aerospace Technology and Management, JATM,* Vol.6, No 4, pp.475-484, Oct.-Dec., 2014
[7] ISO 21940-11:2016 *Standard Mechanical vibration — Rotor balancing — Part 11: Procedures and tolerances for rotors with rigid behavior*